ACTA
PROTOZOOLOGICA

Acta Protozool. (2012) 51: 87–107
http://www.eko.uj.edu.pl/ap
doi: 10.4467/16890027AP.12.008.0512

Effects of Roscovitine on Schedule of Divisional Morphogenesis, Basal Bodies Proliferation and Cell Divisions in *Tetrahymena thermophila*

Janina KACZANOWSKA[1], Mauryla KIERSNOWSKA[1], Hanna FABCZAK[2], Szymon KACZANOWSKI[3] and Andrzej KACZANOWSKI[1]

[1]Institute of Zoology, Faculty of Biology, Warsaw University, Poland; [2]Nencki Institute of Experimental Biology, Warsaw, Poland; [3]Institute of Biochemistry and Biophysics, Warsaw, Poland

Summary. During cell cycle of a ciliate *Tetrahymena thermophila* the divisions of micro- and macronucleus, cortical morphogenesis and cytokinesis are temporarily coordinated. Cortical morphogenesis begins with proliferation of the new ciliary basal bodies (BBs) within meridional cortical rows of ciliary BBs, and with the local proliferation of BBs, which form the new oral apparatus (OA2), positioned subequatorialy and destined for prospective posterior daughter cell (opisthe). Prior to cytokinesis, two prospective daughter cells are of equal size and show metamery of their cortical patterns. We studied effects of 20 μM roscovitine (an inhibitor of several cyclin-dependent kinases) on the cell cycle progression of *T. thermophila*. We showed that roscovitine delayed cell division, delayed or arrested macronuclear division and induced increase of cell size and the number of BBs in the cortical rows. The increase in the number of BBs in cortical rows induced cell elongation which was proportional to the increase in cell surface area. There was uncoupling between this BBs proliferation which is continued during prolonged cell cycle and delayed cytokinesis, what resulted in topological alteration of the respective positions of the OA2 and of the contractile vacuole pores (CVPs). In roscovitine treated cells, the new OA2 was positioned subequatorialy, but the fission zone was shifted posterior to the equatorial plane of the cell and positioned across and in the extreme cases behind of the new OA2. This resulted in the formation of a large proter and small size opisthe. The roscovitine treatment induced a formation of a plethora of phenotypes of postdividing cells. We found that irrespective of changes in divisional morphogenesis induced by roscovitine treatment, all mature BBs were associated with the cdc14-like phosphatase. Taken together all these data indicate that during cell cycle of *T. thermophila* the normal morphology of the daughter cells depends on the proper division of micro- and macronucleus and on temporal control of BBs proliferation along the longitudinal rows, during OA2 stomatogenesis and during selection of BBs involved in differentiation of apical BBs (couplets) and cell division.

Key words: *Tetrahymena*, roscovitine, basal bodies, morphogenesis, macronucleus, cdc14p.

Address for correspondence: Janina Kaczanowska, Institute of Zoology, Faculty of Biology, Warsaw University, Miecznikowa 1, Warsaw 02-096. Poland. E-mail: kaczan@biol.uw.edu.pl

INTRODUCTION

The cell cortex of *T. thermophila* consists of 17–21 antero-posterior rows of ciliated and non-ciliated basal bodies – BBs (Shang *et al.* 2005) and longitudinal microtubule bundles (LMs) parallel to the rows. The oral apparatus (OA1) is positioned subapically, the contractile vacuole pores (CVPs) and the cytoproct (CYT) are located in the posterior cell cortex at the determined position of the cell circumference (reviewed in Frankel 2000). In contrast to the division in metazoan cells, the division in *Tetrahymena* involves the reorganization of the parental cortical pattern into dual metameric patterns of daugther cells. The polarity of the BBs rows (controlled by the Mob1 polarity marker appearing prior to cell division in posterior BBs rows in both forming daughters, Tavares *et al.* 2012) does not change during cell divisions. Under normal culture conditions, during each cell cycle, the cell develops the new oral apparatus (OA2) for the posterior daughter (opisthe) and the new contractile vacuole pores (CVPs) and the cytoproct (CYT) for the anterior daughter (proter) (reviewed in Frankel 2000), and opisthe and proter are the same size (Lynn 1977, Kaczanowski 1978, Frankel *et al.* 1981, Nelsen *et al.* 1981). At the start of OA2 stomatogenesis, the BBs proliferate laterally to the left of the right ventral postoral row #1 to form an "anarchic field" of BBs. The cortical area of the anarchic field and mature OA1 are deprived of the epiplasmic antigen (Williams *et al.* 1987, ~~Williams *et al.*~~ 1990). Subsequently, the BBs within the anarchic field are assembled into the oral membranelles of the OA2, with programmed resorption of some of them, followed by development of structures of oral pouch and cytopharynx (Lansing *et al.* 1985, Williams *et al.* 1986, Takeda *et al.* 2001, Gould *et al.* 2011).

Prior to cell division, the cortical rows are transected at the cell equator around its circumference with the katanin (Sharma *et al.* 2007). This equatorial zone of gaps in the BBs rows is called the fission zone. The equatorial positioning of the fission zone is determined at early stages of oral morphogenesis ~~by~~ by the proximal end of the OA2 primordium (Nanney 1975; Kaczanowski 1978; Numata and Gonda 2001; Shang *et al.* 2002, 2005). The appearance of the fission zone (Nelsen *et al.* 1981, Kaczanowska *et al.* 1993, Kaczanowska *et al.*1999, Brown *et al.*1999, Thazhath *et al.* 2002, Thazhath *et al.* 2004) is followed by the wave of ciliation of the 12 basal bodies of cortical rows, located posterior to the fission zone (Frankel *et al.* 1981).

In most ciliary rows two BBs located posterior to the fission zone differentiate into couplets: anterior, unciliated BB ("stumpy" BB) and next ciliated BB. These couplets form so called "couronet" of the apex of the opisthe. The "stumpy" BBs are directly involved in the formation of the apical ring of filaments (ARF) for the opisthe cell (Diogon *et al.* 2001) and are implicated in formation of contractile fission ring during cytokinesis (Jerka-Dziadosz 1981, Numata *et al.* 1995). The differentiation of couplets depends on the protein p85 and its interaction with Ca^{2+}/calmodulin (Gonda *et al.* 1999, Gonda and Numata 2002). It is likely that the modification of the p85 protein depends on product of the TTHERM_00590090 gene [named TGD U LL61625(309) Bradley U and, renamed CMB1 by Frankel 2005].

The final fission line of furrowing (Jerka-Dziadosz *et al.* 1995, Kaczanowska *et al.* 1999) is specifically labelled by the antibody directed against the subepiplasmic 64-kDa protein (fenestrin) (Nelsen *et al.* 1994). Appearance of the fission line is involved in organization of the fission contractile ring underneath cortical membrane (Gonda and Numata 2002, Shirayama and Numata 2003, Wilkes and Otto 2003, Williams *et al.* 2006). Trafficking of the endosomes (Baluska *et al.* 2006, Zweifel *et al.* 2009) provides components for new cell surface during cell growth and cytokinesis (Smith *et al.* 2004, Williams *et al.* 2006, Kushida *et al.* 2011). In ciliates, generation of tensional forces is involved in separation of daughter cells (Yasuda *et al.* 1980, Kaczanowska *et al.* 1995). It has been also shown that, the β tubulin mutation selectively uncouples macronuclear division and cytokinesis (Thazhath *et al.* 2002, Smith *et al.* 2004). However, our understanding of the control of the positioning of the OA2, the new CVPs and the couplets, and control of the proliferation of BBs in cortical rows during divisional morphogenesis of *T. thermophila* remains vague. Some checkpoints (reviewed Cole and Sugai 2012) operating during *Tetrahymena* cell cycle synchronize three different developmental pathways: (i) the replication of DNA and amitotic division of macronuclei (Kovacs and Pallinger 2003, Kushida *et al.* 2011, Gotesman *et al.* 2011, Sugita *et al.* 2011), (ii) the sDNA and mitosis of micronucleus, and (iii) the cortical morphogenesis. These three pathways control together cell division machinery ~~dividing cells~~ (Krzywicka *et al.* 1999, Kovacs and Pallinger 2003, Smith *et al.* 2004, Shang *et al.* 2005).

In this study we asked the question whether the cell size, number of BBs in cortical rows, positioning of the

OA2, and CVPs in dividing cells may be experimentaly modified. For this purpose we used low dose of roscovitine, an inhibitor of many cyclin dependent kinases, which delays progression of cell cycle in metazoan cells (Meijer *et al.* 1997, Whittaker *et al.* 2007). We were also interested in the effects of the roscovitine on the co-ordination of nuclear and cortical events in *Tetrahymena*, since in Metazoa roscovitine induces overpassing of the cyclin-dependent spindle checkpoint in the cells arrested at anaphase (D'Angiolella *et al.* 2003).

In many types of cells, roscovitine also inhibited phosphorylation of the ß-tubulin by the cyclin dependent kinase which is prerequisite for the assembly of microtubules in these cells (Fourest-Lieuvin *et al.* 2006). Kamijo *et al.* (2006), Steere *et al.* (2011) showed that in metazoan cells this inhibitor induces cell cycle delay and unequal cell division but it does not prevent the extra-amplification of centrioles. Because the BBs of *Tetrahymena* are able to substitute the centrioles in the extracts of metazoan cells (Heidemann and Kirschner 1975) we wanted to know how the roscovitine treatment affects the BBs proliferation involved in general pattern formation in dividing *Tetrahymena*.

MATERIALS AND METHODS

Materials

Tetrahymena thermophila CU428.1 mtVII was provided by Dr. J. Gaertig, and by Tetrahymena Stock Center (Cornell University). Growth culture medium contained 1% proteoso-peptone (Difco) supplemented with: 0.1% yeast extract, 0.2% glucose, 90 µM Fe EDTA, streptomycin and penicillin. Before the experiments, 10 ml of culture medium was inoculated with 100 µl of stock culture, in plastic Petri dishes (9 cm diameter), grown at 31°C. The cells were transferred daily during next 3 days.

Chemicals

Roscovitine was purchased from Sigma-Aldrich (catalog number R7772). The 10 mM stock solution of the roscovitine in DMSO was prepared according to Kamijo *et al.* (2006) and was added at final concentration of 20 µM to cell the growth medium.

Immunostaining of centrin, fenestrin and anti-B epitopes

Monoclonal antibodies: anti-centrin 20H5 (1:1200, a gift from Dr. J. L. Salisbury) and anti-fenestrin (mAb 9A7, 1:40, a gift from Dr. J. Frankel) were used according to Kaczanowski and Kiersnowska 2011 and Nelsen *et al.* 1994, respectively. Immunostaining with the rabbit antiserum against B component of epiplasm of *Tetrahymena* (1:80, a gift from D. E. Williams) was followed the protocol described by Williams *et. al.* (1987). Immunostained cells were mounted with Dako Cytomation Fluorescent Mounting medium (DAKO) or with Ultra Cruz™ mounting medium containing DAPI (Santa Cruz Biotechnology). For tests of nuclear division and their configurations in dividing cells, the fixed cells were directly placed on polylisine slides.

Immunostaining and immunogold labelling of cdc 14 epitopes

The monoclonal anti cdc14A antibody was purchased from Sigma-Aldrich. The cells were fixed 10 min. with 2% formaldehyde (Electron Microscopy Sciences) in PHEM buffer (Schliva and Blerkom 1981) containing Triton X-100 (0.15%). Next, the cells were washed with PBS and fixed for 30 min. (on ice) in 35% ETOH with 0.3% Triton X-100. Double fixed cells were washed: 2× with PBS and 3×30 min. with PBS containing 0.3% BSA and 0.05% Tween 20. After overnight incubation with anti-cdc14A antibody (4°C, dilution: 1:75) and washing with PBS/BSA/Tween20 (3×30 min.) the cells were treated (2 h at 30°C) with Alexa Fluor 488 donkey anti-mouse IgG (dilution 1:1000, Invitrogen, Molecular Probes), for fluorescent microscopy or with anti-mouse IgG gold conjugate (5 nm, dilution 1:10, Sigma), for immunogold labelling. Immunostained cells were washed with PBS and mounted with Dako Cytomation Fluorescent Mounting medium (DAKO). Immunogold labelled cells were washed with PBS/BSA/Tween 20 (4×15 min.) and 30 min. postfixed with 0.5% glutaraldehyde (Electron Microscopy Sciences). After washing with PBS and destilled water the cells were embeded in 1% agarose. Dehydratation was done in a graded series of ethyl alcohols, followed by aceton. The samples were embeded in epoxy resin. The ultrathin sections were stained with saturated aqueous uranyl acetate for 5 min.

Immunostained cells and the ultrathin sections were analyzed under Nikon Eclypse E-600 microscope equipped with with VDS camera and JEOL 1200Ex electron microscope, respectively.

For cell measurements the VDS camera and Lucia 4.6 image analysing program were used. The microphotographs were edited with the Adobe Photoshop program.

Immunobloting

Cell fractionation, electrophoresis and Western blotting of the cdc 14 protein were performed according to the protocol of Kaczanowska *et al.* (2008).

RESULTS

Cortical divisional morphogenesis in control *Tetrahymena thermophila*

The oral apparatus (OA) of *Tetrahymena* (Fig. 1) consists of oral mebranelles: undulans membrane (UM) on the right margin of the oral pouch and three adoral membranelles (M1–M3) inside the pouch (reviewed in Frankel 2000). On its right side there is microtubular oral ribs (Kiersnowska and Golinska) with material labelled with anti-centrin antibody – oral crescent

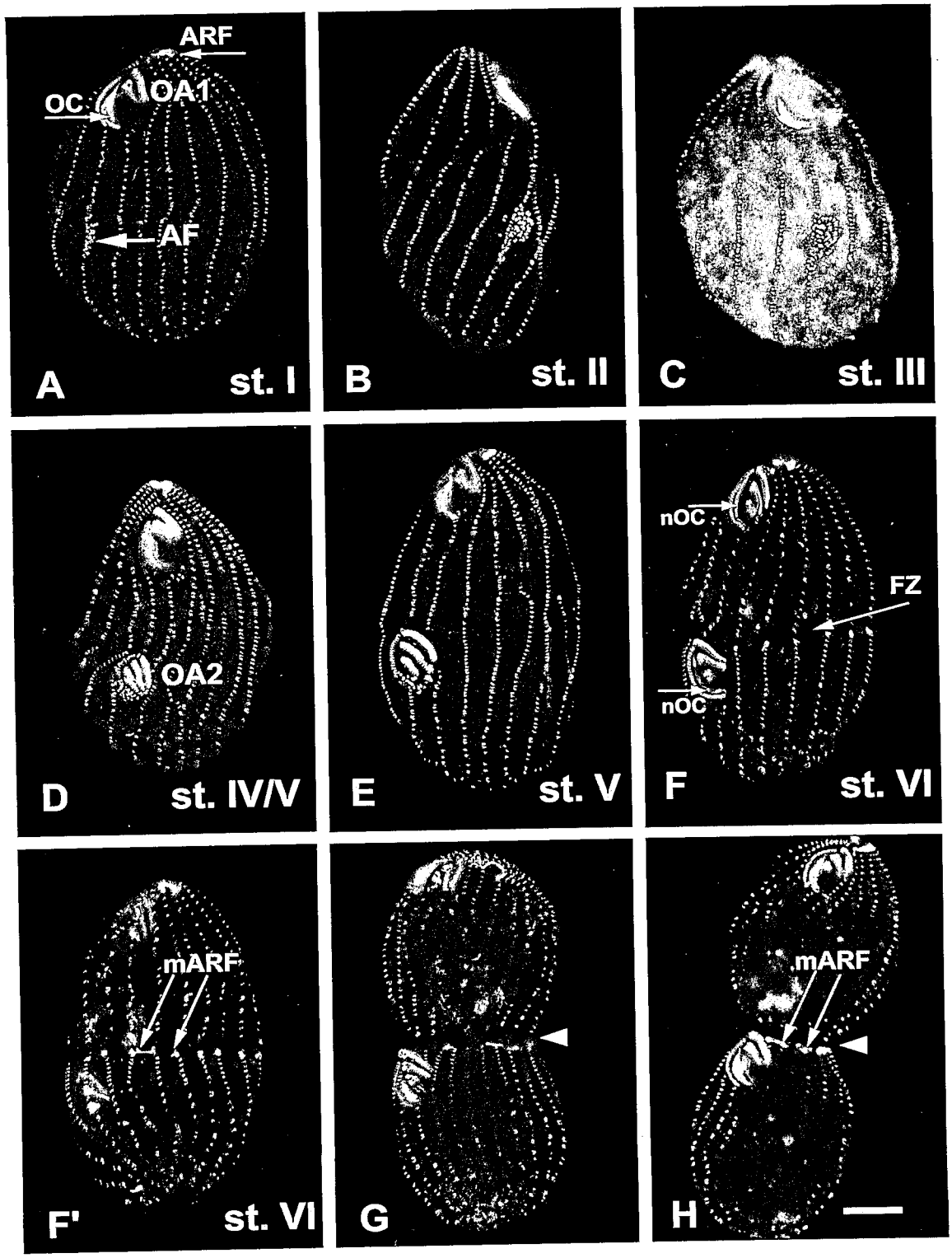

Fig. 1. Divisional [illegible]ogenesis and cytokinesis in untreated (control) *T. thermophila*. Cells were immunostained with the anti-centrin 20H5 antibody. **A–F** stomatogenesis, stages I–VI; **G–H** cytokinesis. AF – an anarchic field, ARF – parental apical ring of filaments, mARF material for new ARF localised on in the proximal ends (couplets of BBs) of cortical rows in opisthe cell, FZ – fission zone, OA1 and OA2 – parental and new oral apparatuses, OC – parental oral crescent, nOC – new oral crescents in both daughter cells. Bar: 10 μm for A–H.

(2) brak objaśnienia i podpisie dla F'

(OC), (Diogon *et al.* 2001, Guerra *et al.* 2003). The oral structures are underlayed with connectives composed with: microtubules (Allen 1967), specific tetrin filaments (Gould *et al.* 2011; Williams 1986; Williams *et al.* 1986, 1987; Honts, Williams 1990) and epiplasmin components (Gould *et al.* 2011).

Nelsen *et al.* (1981), Bakowska *et al.* (1982) and Lansing *et al.* (1985) distinguished six stages of development of new oral apparatus (OA2) in *Tetrahymena*. The development of the OA2 begins with proliferation of BBs in the middle region of row #1 and to the left of this row (Fig. 1A, stage I) that results in the formation of an anarchic field of BBs. The anarchic field is consolidated (Fig. 1B, stage II) and its BBs are subsequently assembled into the oral membranelles (Fig. 1C–E, stages III–V). Internal pattern of oral apparatus is established during the stage V. At the stage V a partial reorganization of the parental OA1 takes place. This involves reorganization of the undulans membrane (UM) and transient disappearance of the oral crescent. Subsequently, the oral crescents re-appear in the old OA1 and in the new OA2 (Fig. 1F). The fission zone and cytokinetic furrow (Fig. 1F–H) are localized in the equatorial region of the cell. The material for new ARF is deposited in the opisthe at the proximal ends of its cortical rows, i.e. on a stumpy basal bodies of the couplets. Its deposition begins prior cytokinesis and starts from the dorsal side (Fig. 1F') and progresses around the cell's circumference (Fig. 1F–G). During furrowing (cytokinesis), the materials deposited at the ends of couplets fuse into the half ring of ARF (Fig. 1H).

Unequal and delayed cell divisions induced with roscovitine

The 10 ml of culture medium with 20 μM of roscovitine was inoculated with 100 μl of the cell culture at a density of 0.5–1×10^6 of cells/ml. The mean doubling time of untreated CU428 cells was about 150–180' in a culture of density of 10–100×10^5 cells/ml. 1.5 h after the transfer of cells to the medium containing roscovitine cells transiently arrested their divisions. After 3 h of the roscovitine treatment the unequal cell divisions were observed with opisthes smaller than proters. After 5 h of the treatment the frequency of dividing cells increased to about 30%. Beginning from the 7th hour of the roscovitine treatment we observed the accumulation of cells completely arrested in cell division. After 24 h of the treatment, the total number of cells increased 2–2.5 times and almost all cells were arrested in cytokinesis and transformed into monster cells. Thus in the presence of roscovitine the cells were able to divide at least once and this division was unequal. The results of anti-centrin immunostaining of CU428 cells grown in the absence and presence of 20 μM roscovitine at 31°C and fixed at 1.5, 3.5 and 5.5 h of roscovitine treatment are presented in Table 1. These data showed that roscovitine trated cells resumed cortical morphogenesis after 3.5 h and 5.5 h treatments showing posteriorly shifted fission zone at the stage VI, and then the cells were cumulated in stage of unequal cytokinesis.

Table 1. Distributions (in %) of divisional morphogenesis stages of *T. thermophila*: untreated (control) and treated with roscovitine.

		Stages of divisional morphogenesis (%):							Ab.		
Samples	N[a]	0	I–IV	V	VI–Reg.	Shift	Cytokinesis[c] Reg.[d]	Shift[e]	Post-divid.		Res.
Control											
1.5–5.5 h	1358	63.3	21.9	6.4	5.1	–	3.3	–	–	–	–
Roscovitine					–	–	–	–			
1.5 h	472	68.2	17.8	6.6					–	1.3	6.1
3.5 h	494	32.2	25.9	6.5	–	10.9	–	18.4	3.2	0.6	2.2
5.5 h	429	19.1	12.8	10.0	–	10.0	–	39.9	6.8	–	1.4

[a]N – number of scored cells; [b]FZ – the fission zone; [c]Cytok. – the cytokinesis; [d]Reg. – the fission zone or fission furrow in the middle of cell, slightly above OA2; [e]Shift – the fission zone or the fission furrow localized across or posterior to the OA2; [f]Ab. Postdivider proters with membranelles of OA2 localized on posterior pole of cell and opisthes with remnants of OA2 membranelles or opisthe without OA; [g]OR – the oral replacement; [h]Res. – the resorption of OA2.

Failure in coordination of nuclear and cortical events induced with roscovitine

During cell cycle of *Tetrahymena thermophila* micronuclear division (anaphase) occurs during the stage V of the cortical morphogenesis. The elongation of the macronucleus, i.e. beginning of its division appears at the stage V and its division is completed prior to cytokinesis (Table 2, Fig. 2A, B). These results were consistent with McDonald (1962), Frankel *et al.* (1976), Wu *et al.* (1988), Smith *et al.* (2004), Kirk *et al.* (2008). In the roscovitine treated cells, some cases of an unequal macronuclear division were observed (Fig. 2C), but in majority of cells the macronucleus was undivided in the stage VI of the cortical morphogenesis and during cytokinesis, in contrast to the control cells. The undivided macronuclei were preferentially segregated into the forming proter and the division of micronuclei was not disturbed by the drug (Table 2, Fig. 2D). These results show that roscovitine affected macronuclear divisions and the coordination of the division of macronucleus and cytokinesis. Normal mitosis of micronuclei was observed but micronuclear divisions were slightly delayed.

Roscovitine induces posterior shift of the OA2 and affects distribution of the OA2 to the posterior daughter cells

The early oral primordia (anarchic field) in roscovitine-treated cells were positioned slightly subequatorialy, i.e. similar as in control cells. However, after 3.5 and 5.5 h of roscovitine treatment the fission zone was shifted posterior, running across the OA2 (Fig. 3A–D) and in extreme cases even posterior to it (Fig. 3E–F'). Some of the proters acquired (at least transiently) entire second mouth (OA2) positioned at their posterior pole and the opisthes remained mouthless. Furrowing in the roscovitine treated cells started with the formation of the fission zone in dorsal cortical rows (Fig. 3A' and B). In forming opisthe the differentiation of couplets of BBs (Fig. 3B) and deposition of ARF material (Fig. 3C–F', mARF) were visible even in the cells with incomplete cytokinesis.

Some cells treated with roscovitine for 3.5 and 5.5 h had an abnormal number and pattern of adoral membranelles at the stages V or VI of stomatogenesis and during cytokinesis (Fig. 3A, C, D). Moreover, at 5.5 h, 28% of the cells in cytokinesis had oral primordia with

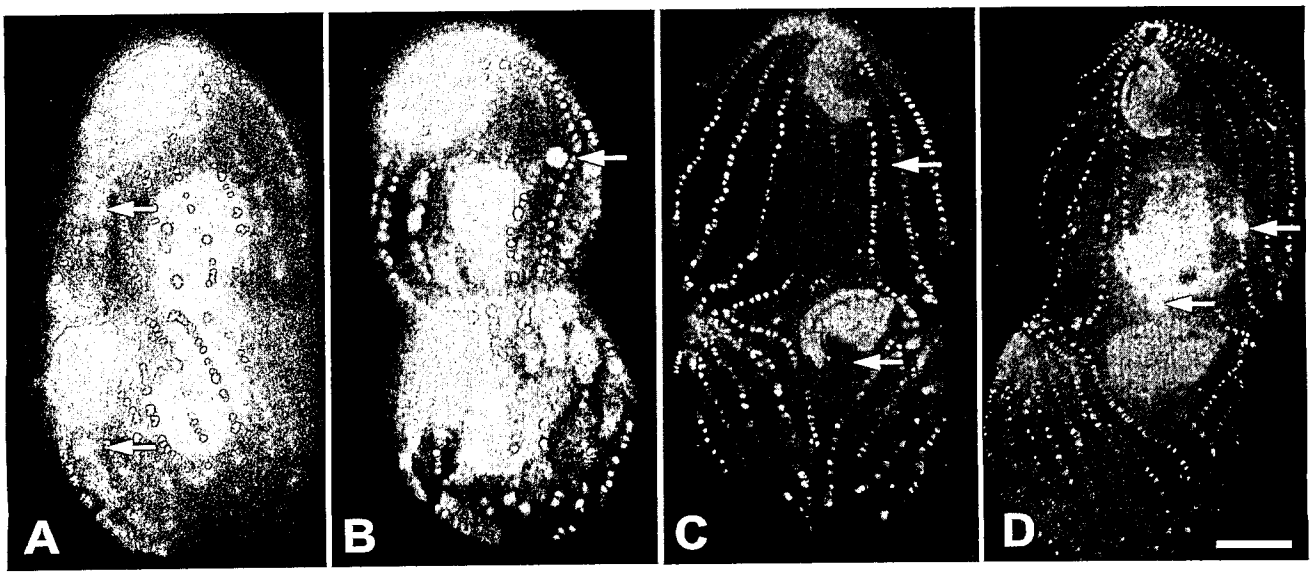

Fig. 2. Localization of nuclei in control and roscovitine treated *T. tetrmophila*. The cells were immunostained with the anti-centrin 20H5 antibody and stained with DAPI. **A** and **B** – control cells in the VI stage of morphogenesis, and [illegible] cytokinesis, respectively; **C** and **D** – roscovitine treated cells (4 h) in the VI stage of morphogenesis and in cytokinesis respectively; arrows – micronuclei (in the C micronucleus in opisthe is out of focus). Bar: 10 μm.

Table 2. Distribution of nuclear configurations scored in late morphogenetic stages and in cytokinesis, after roscovitine treatment.

	N	NUCLEAR CONFIGURATIONS IN %				
		CONTROL				
				proter		
				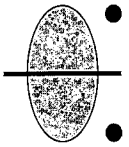	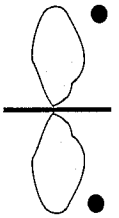	
				opisthe		
stage V	78	40	42	18		
stage VI	75			32	68	
cytokineis	56				100	
		AFTER 3.5 H OF THE ROSCOVITINE TREATMENT				
				proter		
		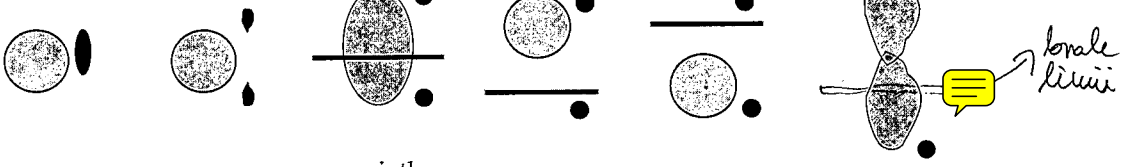				
				opisthe		
stage V	50	62	38			
stage VI	65			45	49	6
cytokinesis	206			17	56	3	24

Gray filled – macronuclei; black filled – micronuclei; horizontal bars – position of fission zone or fission furrow in relation to the nuclei; N – sample sizes.

uncompleted assembly of oral membranelles. In some cases the small field of unassembled BBs remained in the posterior part of the OA2 (Fig. 3C, arrow). Nevertheless, the oral crescent developed in OA2 independently of the acquired pattern of oral membranelles.

Cortical pattern of post-divider cells after roscovitine treatment

In result of unequal cell divisions the postdividers cells identified as proters might receive the ectopic OA2 oral apparatus or only a part of the OA2 structures, localized on their extended posterior pole (Fig. 4A and A'). The cells with extended posterior pole (smaller than other nondividing cells) but without the OA2 were also observed (data not shown). It suggested that an ectopic OA2, or the some structures of OA2 transfered to the proter were lost. The other small cells (smaller than proters, Fig. 4B–E') with apicaly located OA, with uncomplete, disorganized oral structures and without oral structures were identified as opisthes, formed in presence of roscovitine. In some of these opistes ARF was localized on dorsal side (Fig. 4B) or was uncompleted (Fig. 4E and E').

The localization of an anarchic field of BBs below regular formed OA2 was observed in some cells (Fig. 4D–E), suggesting their entrance into an oral replace-

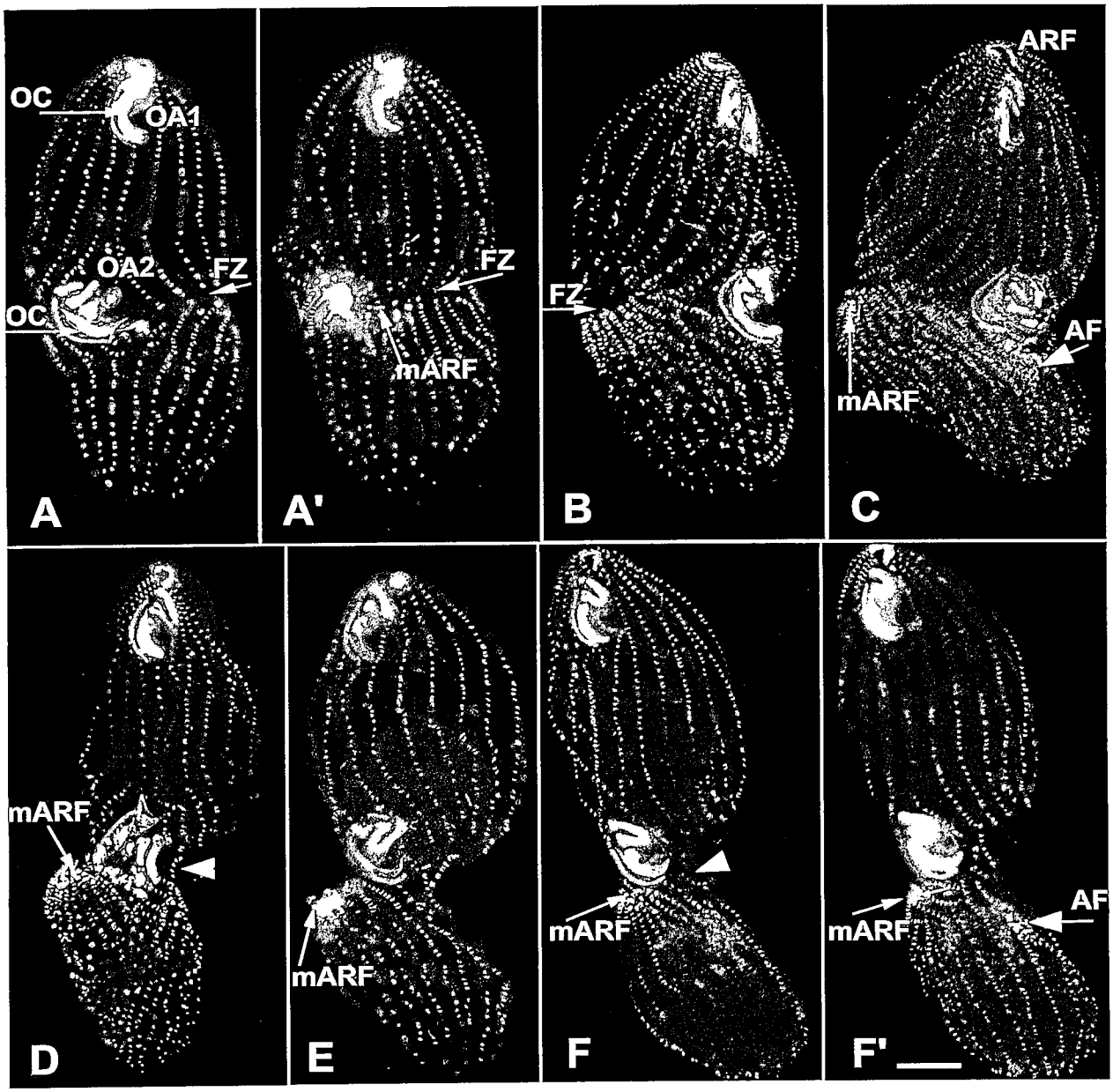

Fig. 3. Divisional morphogenesis and cytokinesis in *T. thermophila* after 5.5 h treatment with roscovitine. Cells were immunostained with the anti-centrin 20H5 antibody. **A–C** – stage VI of divisional morphogenesis; **D–F'** – cytokinesis; **A** and **A'** – ventral and dorsal views of the same cell. Other explanations as in Fig. 1. Bar in F': 10 μm for A–F'.

ment pathway. Morphology of some opisthe (Fig. 4 E and E') strongly suggested that the rigid oral apparatus, might pinch off due to asymmetric tensional forces of furrowing operating during cell division.

Morphometric study on correlation of cell growth and proliferation of basal bodies

The spatial parameters of dividing cells in control, untreated *T. thermophila* and in cells treated with roscovitine are summarised in Table 3. Roscovitine treatment resulted in increased cell size and the number of BBs per

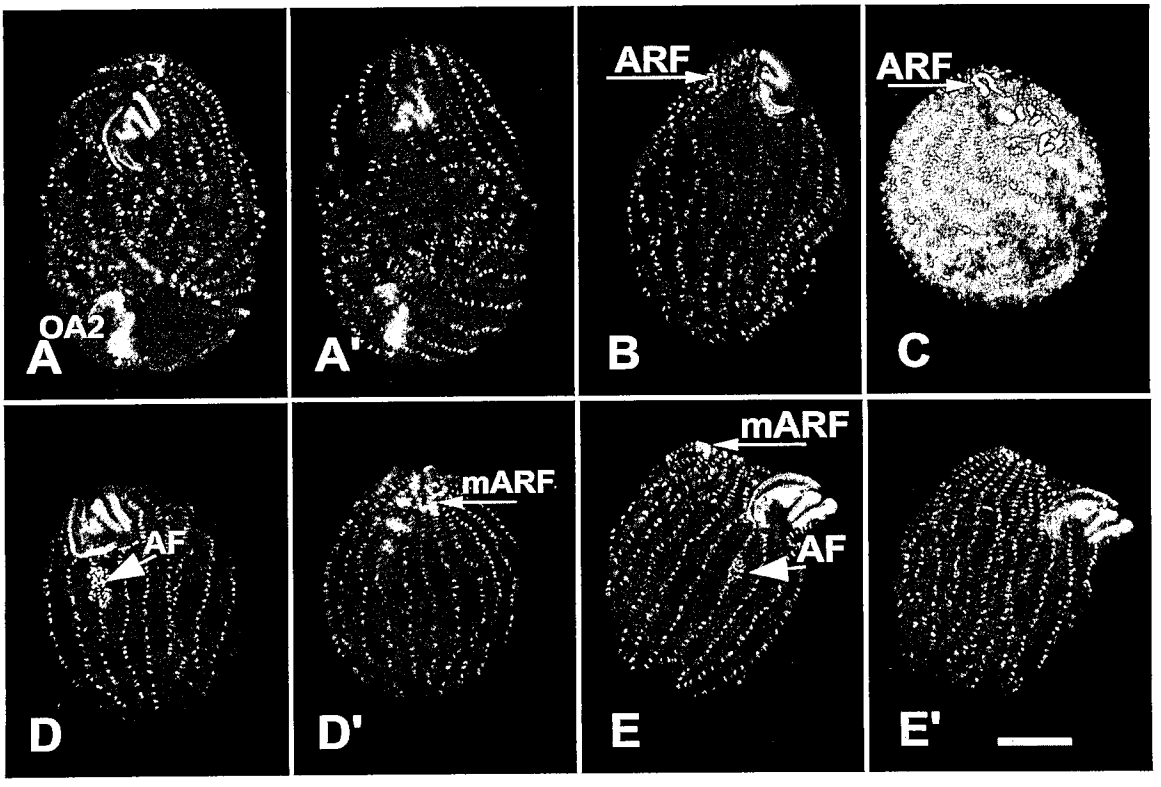

Fig. 4. Postdiv ells after 5.5 h of roscovitine treatment. Cells were immunostained with anti-centrin 20H5 antibody. **A** and **A'** – ventral and dorsal view of the same proter cell with remnants of the OA –**C** opisthe cells, **B** – opisthe with ARF on dorsal side, **C** – opisthe with remnan oral structures; **D** and **D'** – ventral and dorsal view of the same cell; **E** and **E'** – ventral and dorsal view of the same opisthe during p ing off of the OA. Other explanations as in Fig. 1. Bar: 10 μm for A–E'.

row. The mean numbers of BBs per ciliary row in control cells were similar to those found by Kaczanowski (1978) and by Kaczanowski and Kiersnowska (2011). Consistent with their results more BBs were present in the ventral rows #2 and #n-1 than in the dorsal row #7 or #8. The 3.5 and 5.5 h of roscovitine treatments resulted in the addition of about 18.5–23 BBs and about 28–33.5 BBs to the cortical rows, respectively. As in control cells more BBs appeared in ventral, than in dorsal rows (the difference even slightly increased). The linear density of BBs (calculated as a mean number of BBs in cortical rows #n-1, #2, and #7, 8/cell length) in control cells was 0.71 BBs per μm of cortical row and it remained roughly unchanged from early stage cortical morphogenesis to cytokinesis (0.76 BB's per μm). In contrast, after 3.5 and 5.5 h of roscovitine treatments the linear density of the BBs in late dividers increased to 0.9 and to 0.99 BBs per μm, respectively. We asked if there is a correlation between the proliferation of the BBs in cortical rows and the increase of cell surface area. To answer this, we estimated the BBs density per μm^2 assuming that the mean number of BBs in ciliary rows #n-1, #2 and #7 represents the mean number of BBs per each cortical row and that the measured cell contains 18 cortical rows. Such estimations showed that the "density" of BBs in proter cells of late dividers in untreated cells and in cells treated 3.5 or 5.5 h with roscovitine was the same, i.e. 0.28 BBs/μm^2, and in the opisthe cells this density increased from 0.28 to 0.35 BBs/μm^2. Thus, roscovitine induced an increase of number of BBs in ciliary rows, was proportional (at least in proters) to the increase of the cell surface area.

Table 3. Morphometry of untreated and roscovitine treated cells: cell sizes, position of OA2, numbers of BBs in chosen rows and BBs density.

Cell Samples		Length (μm)	Width (μm)	Distance Apex – OA2 (μm)	Number of bbs in ciliary row: n-1	2	7 or 8	Mean number of BBs in row/cell length (BBs/μm)	Density of BBs = number of BBs/cell surface area[d] (BBs/μm²)
Early dividers									
Control N = 11									
	mean	46.5	29.6	23.8	33.7	38.9	26.7	0.71	0.28
	CV[a]	3.1	9.5	7.0	5.2	4.5	6.5		
Roscovitine 3.5 h									
N = 11	mean	49.5	35.5	25.5	45.2	50.1	38.2	0.90	0.29
	CV[a]	5.0	7.0	9.8	11.5	7.3	13.3		
Number of extra BBs added[e]					11.5	11.2	11.5		
Late dividers									
Control N = 13									
proter	mean	29.9	26.2	31.4	21.5	25.4	19.0	0.73	0.28
	CV[a]	9.2	10.6	10.0	10.0	8.9	9.8		
opisthe	mean	27.7	25.9		22.0	26.5	17.2	0.79	0.28
	CV[a]	8.1	6.5		9.8	10.8	8.9		
	Σ mean	57.6			43.5	51.9	36.2	0.76	0.28
	CV	7.8			8.5	8.8	5.5		
Roscovitine 3.5 h									
N = 33									
proter	mean	38.7	32.5	35.9	37.8	38.5	30.6	0.887	0.29
	CV[a]	12.7	8.4	8.9	20.6	19.2	16.3		
opisthe	mean	29	28.2		28.8	33.4	24.1	0.92	0.35
	CV[a]	14.7	10.3		15.9	19.5	15.0		
	Σ mean	67			66.6	71.9	54.7	0.90	0.29
	CV[a]	12.2			13.7	16.8	12.5		
Number of extra BBs added[e]					23.1	20.0	18.5		
Roscovitine 5.5 h									
N = 10									
proter	mean	40.8	37.4	36.7	43.9	44.1	33.7	0.994	0.27
	CV[a]	13.2	11.2	14.0	18.7	11.1	33.5		
opisthe	mean	33.3	28.8		33.1	37.1	27.4	0.977	0.34
	CV[a]	6.0	16.0		16.8	27.5	17.3		
	Σ mean	74.1			77.0	81.2	61.1	0.986	0.30
	CV[a]	8.7			12.9	11.9	28.1		
Number of extra BBs added[e]					33.5	29.3	28.2		

[a]CV coefficient of variance; [b]mean value of BBs was calculated for rows: n-1, 2, and 7 or 8; [c]number of BBs per cell was calculated as mean values of BBs per row × 18 (the mean number of ciliary rows); [d]surface area of prospective proter and opisthe cell was calculated using their length and width values and asssuming, that the anterior half of the image of the proter was elipse, posterior half of the image was rectangle and vice versa anterior half of the image of the opisthe was; [e]number of extra BBs added was calculated by substracting numbers of BBs scored in control cells from numbers scored after roscovitine treatment for a given cortical row.

Morphometry of cell size, positioning of the OA2 and the fission zone in control and roscovitine treated cells

During roscovitine treatments, the cells delayed in cytokinesis increased their sizes beyond the limits observed in control dividing cells. This difference was moderate in early dividers after 3.5 h of the roscovitine treatment and increased in late dividers after 5.5 h of the treatment. The topological alteration of the positions of the OA2 and fission line in control and roscovitine treated cells are presented in Fig. 5 (upper panel). In both early and late control dividers, the anterior end of oral primordia was positioned slightly subequatorialy, i.e. the distance from the cell [illegible] to proximal end of

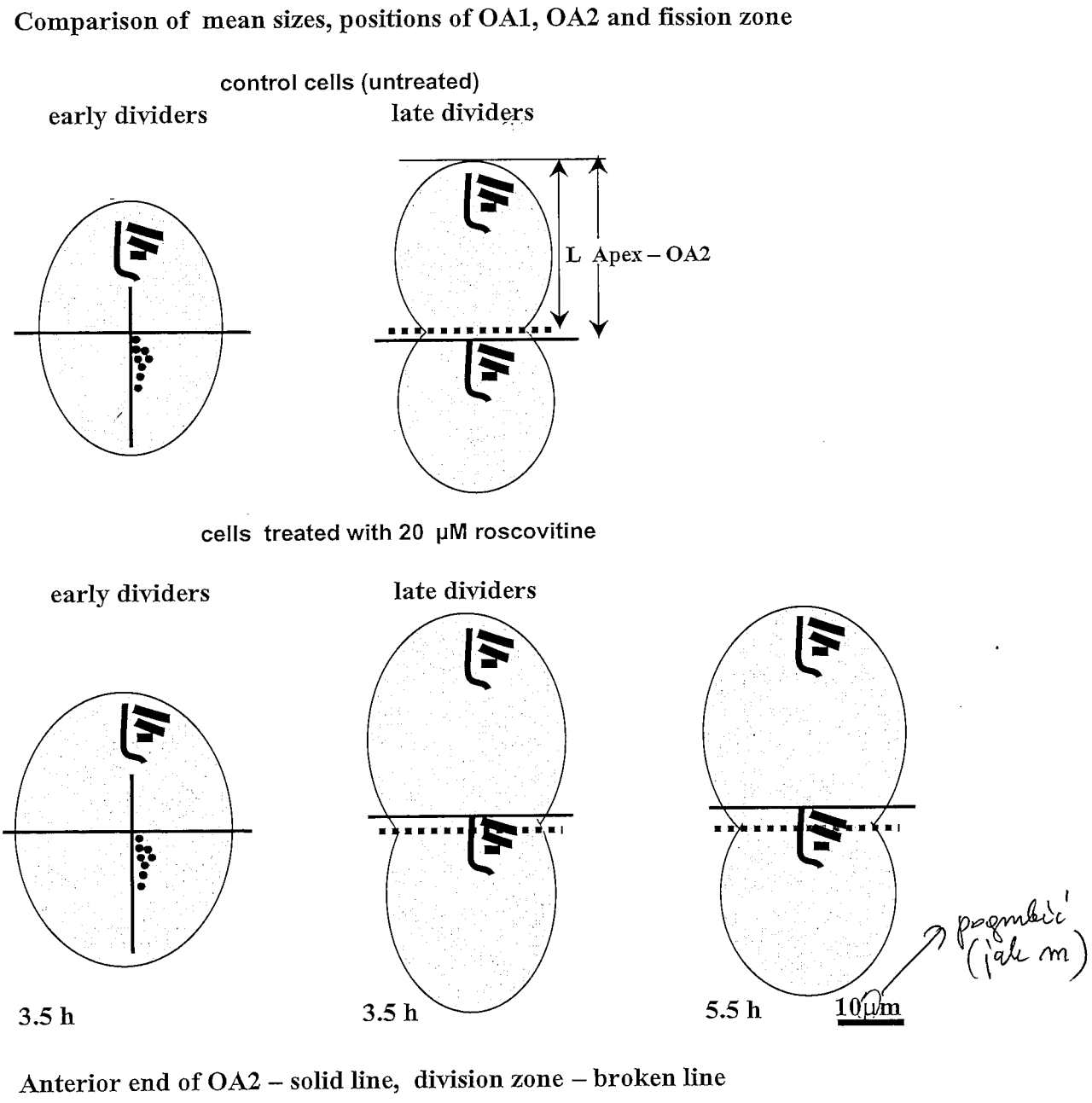

Fig. 5. Mean cell sizes, positions of OA1, OA2 and fission zone in control and in roscovitine treated cells. Upper panel: early and late control dividers, lower panel: early dividers after 3.5 h roscovitine treatment, late dividers after 3.5 and 5.5 h roscovitine treatment. The shape of cells is represented by elipses. Solid horizontal lines – cells "equator", dotted horizontal lines – positions of the fission furrow. All sizes and distances were drawn to the same scale. Bar: 10 μm. The measurements represent means of at least 10 specimens for each cell sample.

the OA2 was slightly longer than the length of the proter. In the roscovitine treated cells (Fig. 5, lower panel) both the early and late oral primordia were also positioned subequatorialy but the fission zone was shifted posterior to cell equator. Thus the distance from the cell apex to proximal end of OA2 was equal or shorter than the length of the proter.

The position of the OA2 in relation to the fission zone was also quantified as a difference between the length of the proter (a distance from the cell apex to

the fission zone) and distance from the cell apex to the proximal end of the OA2 (Fig. 6). In control cells the distance from apex to the OA2 is slightly longer than the length of the proter, because the OA2 is positioned slightly posterior to the fission zone. Hence the difference between length of the proter and the distance from A to the OA2 has negative value. In contrast after roscovitine treatment the distance from cell apex to OA2 is shorter than the length of the proter and the difference between length of the proter and the distance from A to the OA2 has positive value. Fig. 6 shows positive correlation between position of the OA2 and the length of the proter, which was increased after the roscovitine treatment.

Labelling of cell cortex with the anti-epiplasm antibody is not affected by the roscovitine treatment

The use the anti-epiplasm B serum to *T. thermophila* cells showed that pattern of epiplasm distribution remained unaffected in *T. thermophila* after the roscovitine treatment despite of abnormalities in late stages of stomatogenesis (Fig. 7). The oral pouches and the fission zone were in roscovitine treated cells were deprived of the component B of epiplasm as in control cells, with the exception of the faint fluorescence associated with membranelles (Fig. 7A, A' and C) consistent with Williams (1986), Williams *et al.* (1990), Kaczanowska *et al.* (1993, 1999). This serum marked deep fibers (DF) of cytopharynx in both OA1 and OA2 (Fig. 7A, A') consistent with Williams (1986).

Immunostaining of fenestrin in roscovitine-treated *T. thermophila*

In control cells, the anti-fenestrin antibody labelled the anterior regions of both daughter cells in a gradient-like pattern, and labelled the OA1, OA2, the CVPs and the cytoproct (Fig. 8A–D). At the stage VI this antigen strongly marked fission line, i.e. posterior margin of the fission zone (Fig. 8B and C), which was consistent with description of Nelsen *et al.* (1994) and Kaczanowska

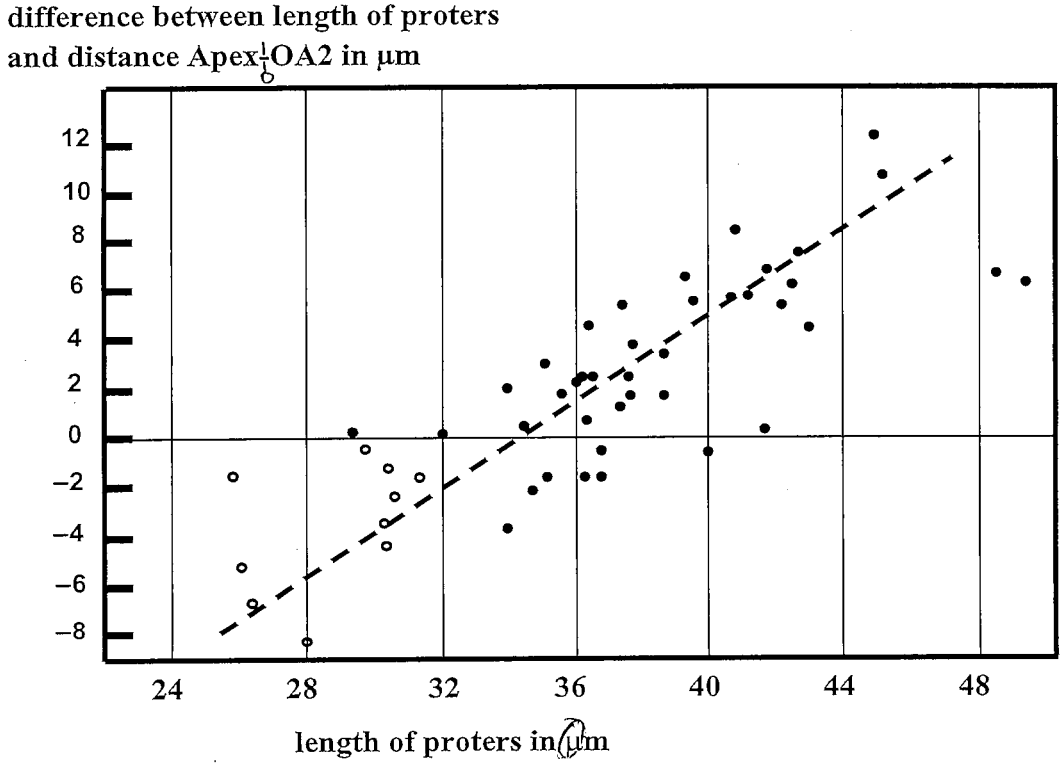

Fig. 6. Correlation of length of proters and shift of the fission zone in relation to OA2 induced by roscovitine in late dividers. The shift of the fission zone was measured as a difference between length of the proters and distance from cell apex to the anterior end of the OA2 (ordinate). Each point in this diagram represent individual cell. Open symbols – untreated cells, close symbols – cells treated with roscovitine for 3.5 and 5.5 h (pooled).

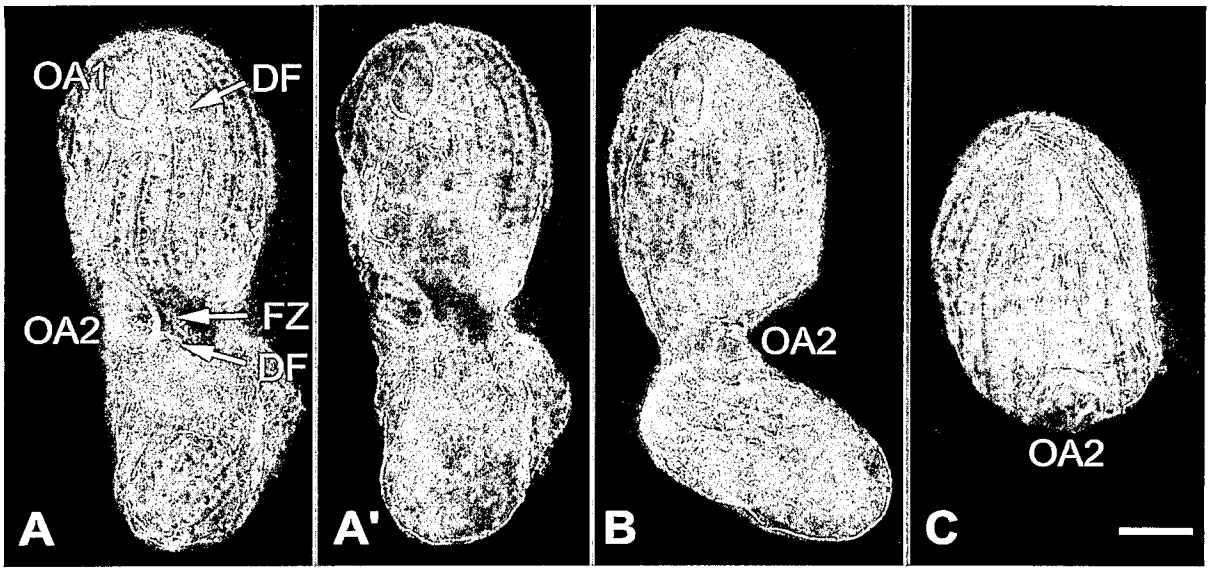

Fig. 7. *T. thermophila* cells immunostained with the antiserum against component B of epiplasm. DF – staining around the deep fibers. Other explanations as in Fig. 1. Bar: 10 μm.

et al. (2003). In roscovitine-treated cells this antibody marked the same cortical structures as in control cells (Fig. 8E–L). Consistent with Nanney (1966) description, the new CVPs in control cells were positioned anterior to the fission line at the same circumferential position as old CVPs (Fig. 8B, arrow head).

After 3.5 h of roscovitine treatment many dividing cells developed new CVPs anterior to the fission line (Fig. 8E and F, arrow head) as in control cells, even though this fission line was posteriorly shifted (Fig. 8G and H, arrow heads). However, in some cells, the roscovitine treatment induced the appearance of the new CVPs posterior to the fission zone (Fig. 8I–L, short arrows) in addition to the CVPs positioned in front of the fisssion zone (Fig. 8I). In some cells the new CVPs were positioned only posterior to the fission zone i.e. in anterior region of the opisthes (Fig. 8J–L). These results showed that during roscovitine treatment the position of CVPs in cells was usually determined prior to the appearance of the fission line, but in some cells an ingrowth of additional cortex in the midle region of cells resulted in posterior shift of the cortical area which was competent to develop the new CVPs and finally these CVPs fell into forming opisthe.

Search in *Tetrahymena* genome for CDH1 gene that might be involved in mitotic exit and search for association of BBs with cdc14-phosphatase

In eukaryotic cells, the coordination of centriole activities during mitotic exit and cytokinesis depends on association of centrioles with the separase and the cdc14-like phosphatase (Sullivan and Uhlmann 2003, Bembenek and Yu 2001, Kaiser *et al.* 2004, Tsou *et al.* 2009, Zineldeen *et al.* 2009, Bembenek *et al.* 2010, Ah-Wong and Judelson 2011) and with an ubiquitin ligase localized to the centrosomes (Freed *et al.* 1999). In Metazoa, the activation of these enzymes is controlled by the CDH1 mitotic exit signal (Queralt and Uhlmann 2008, van Leuken *et al.* 2009, Steere *et al.* 2011).

All mature BBs in Tetrahymena are associated with the CDK1 homologue (Zhang *et al.* 2002). On the other hand we were unable to find a gene(s) encoding the protein of the CDC 25 phosphatase in the *Tetrahymena thermophila* genome. The separase in *Tetrahymena* is encoded by the gene TTHERM-00297160-C50 (Eisen *et al.* 2006, Pearson and Winey 2009). The homologue of the yeast CDH1 gene is also present in *Tetrahymena* genome (see below). Such data prompted us to search in *Tetrahymena* genome for the cdc14 homologue and to test its putative associations with BBs during cell cycle.

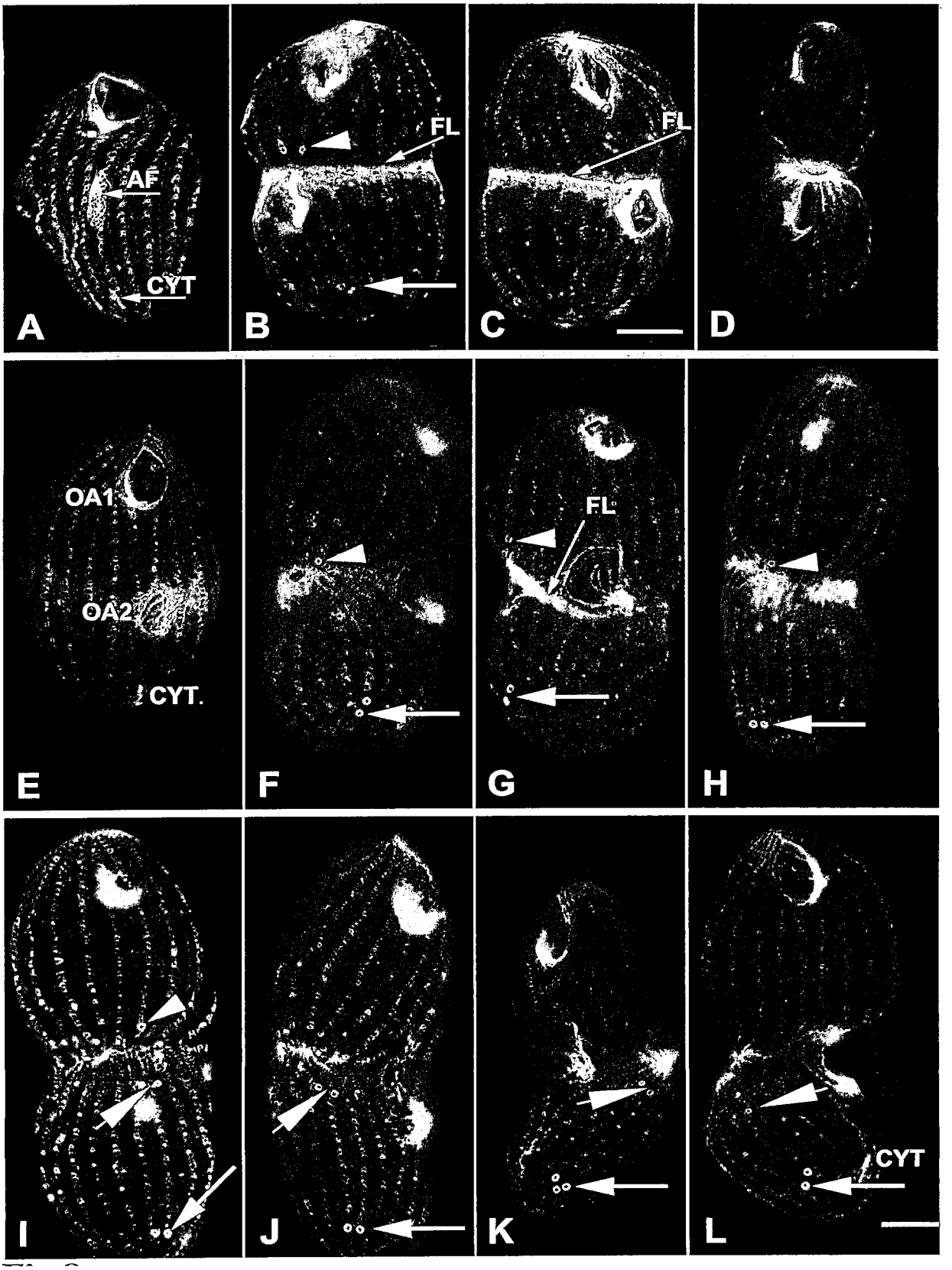
AF
CYT
A
FL
B
FL
C
D
OA1
OA2
CYT.
E
F
FL
G
H
I
J
K
CYT
L

Search for a Cdc14 homologue in *Tetrahymena* genome and presence of putative cdc 14 protein in vicinity of all BBs

To search for a homologue of cdc14p dual phosphatase we used the CDC14 of yeast as a query (uniprot ID CDC14_YEAST) and we used blastp homology search against *Tetrahymena* preliminary prediction of proteome using a TIGR www server http://tigrblast.tigr.org/er-blast/index.cgi?project=ttg. One of the hypothetical orfs is highly homologous (id 14558) ~~to gene~~ for cdc14 gene and homology was detected with an expected value of 8e–53. We used reciprocal blastp against uniprot database (using embl www server http://www.ebi.ac.uk/blastall/index.html?) and the homology with gene CDC14_YEAST was confirmed by a very good expected value 6e–45. We concluded that *Tetrahymena* contains at least one orthologue of CDC14-like phosphatase.

Antibody directed against human ~~Cdc~~14A protein (Wu *et al.* 2008) labelled all BBs: including apical couplets, oral structures and also oral connectives (data not shown) of non-dividing and dividing *Tetrahymena* cells (Fig. 9A–D). The diffused labelling was also observed in macronucleus, but not in the micronucleus. The cortical organelles such as cytoproct, contractile vacuole pores, and ARF remained unlabelled. The same pattern of labelling of all BBs was observed in cells treated for 4 h with roscovitine (data not shown). Western blot analysis identified two protein bands with molecular weight about 65.9 kDa and 51.7 kDa (Fig. 10).

Immunogold labeling revealed the presence of cdc14-like protein around the distal part of BBs both in cortical rows (Fig. 11 A and B), in oral membranelles, and in connective filaments between BBs of oral membranelles (Fig. 11 C). These immunolabellings indicated the peribasal associations of BBs with ~~Cdc~~14-like ~~phosphatase~~.

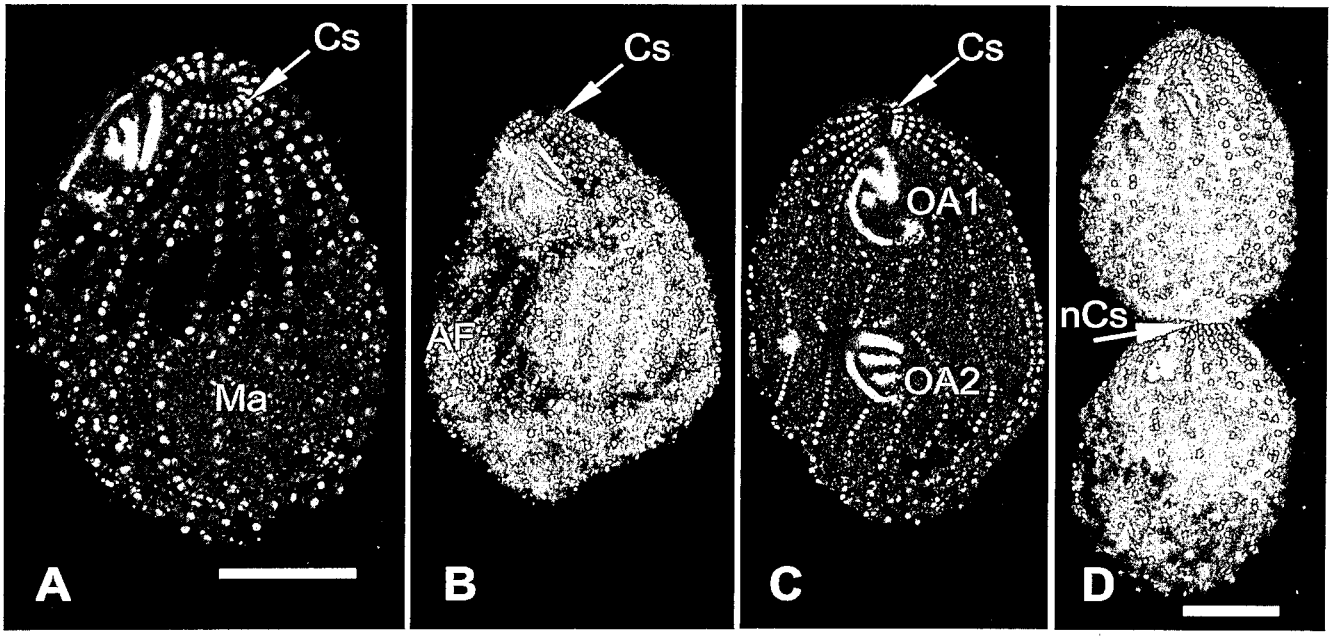

Fig. 9. *T. thermophila* c[illegible]mmunostained with monoclonal anti-cdc14A antibody. Cs and nCS – apical couplets of basal bodies for pro[illegible] and opisthe, respectively. Other explanations as in Figs 1 ~~and~~ 8. Bar: 10 μm, bar in D for B–D.

Fig. 8. *T[illegible]hermophila* cells immunostained with the anti-fenestrin antibody. **A–D** – divisional morphogenesis and cytokinesis of control cells; **E–L** – divisional morphogenesis and cytokinesis of cells treated 3.5 h with roscovitine treatment. CYT – cytoproct, FL – fission line, ~~arrows – parental CVPs~~ long arrows – parental CVPs, arrowheads – new CVPs positioned anterior to the fission zone, short arrows – new (ectopic) CVPs positioned posterior to the fission zone. ~~FL – fission line, CYT – cytoproct~~. Other explanations as in Fig. 1. Bar: 10 μm, bar in C for A–C, bar in L for D–L.

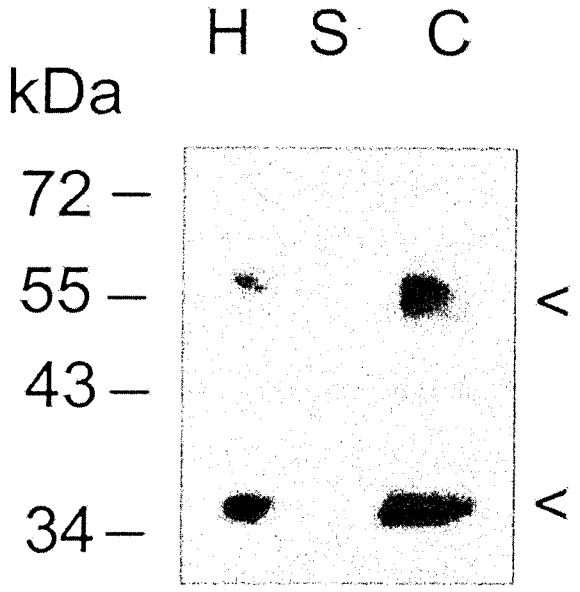

Fig. 10. Western blot of *T. thermophila* fractions with monoclonal antibody anti-cdc14A. H – homogenate, S – supernatant, C – cortical fraction (pellet).

Search for CDH1 co-activator in Tetrahymena genome

We used CDH1 of yeast as a query (uniprot ID CDH1_YEAST) and we used blastp homology search against *Tetrahymena* preliminary prediction of proteome using a TIGR www server http://tigrblast.tigr.org/er-blast/index.cgi?project=ttg. One of the hypothetical orfs is highly homologous (id 27629) to CDH1 and homology was detected with expected value 1.3e–85. We used reciprocal blastp against uniprot database (using embl www server. http://www.ebi.ac.uk/blastall/index.html?) and the homology with gene CDH1_YEAST was confirmed by a very good expected value 9e–86. This indicates that *Tetrahymena* contains CDH1 orthologue.

DISCUSSION

T. thermophila cells show very little variation in cell size, shape and the cortical pattern at the same morphogenetic and cell cycle stages, consistent with Nanney (1966, 1975, 1982). However, the cortical pattern in *T. thermophila* is affected by many genetic mutations (Smith *et al.* 2004, Frankel 2008, Kirk *et al.* 2008, Cole and Sugai 2012) and by experimental treatments (Fran-

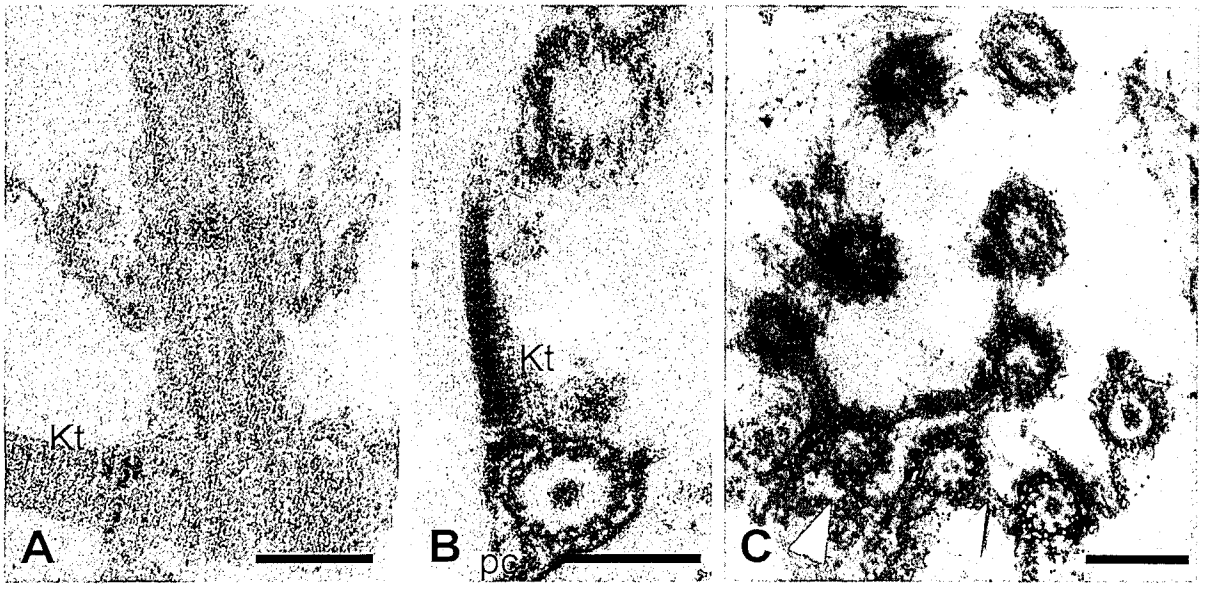

Fig. 11. Cortical structures of *T. thermophila* immunogoldlabelled with anti-cdc14A antibody. **A** – longitudinal section of the ciliated basal body; **B** – transversal section of the fragment of the cortical row; **C** – section at the level of basal bodies of oral membranelle. Kt – kinetodesmal fiber, pc – postciliary microtubules, arrowhead – filamentous material. Bar: 1 μm.

kel and Nelsen 2001, Frankel *et al.* 2001, Smith *et al.* 2004). The effects of roscovitine on the cell cycle and morphogenesis in *T. thermophila* are summarized in Table 4. Roscovitine induced delayed cell division, failure in macronuclear division, increase of cell size beyond the limits observed in control cells and posterior shift of the fission zone.The undivided macronucleus was preferentially segregated to the proter cell. This uncoupling of nuclear and cell division suggest, that roscovitine affected the microtubule – related functions.

The posterior shift of the fission zone and of the fission furrow induced with the roscovitine were correlated with the size increase of dividing cells. During normal morphogenesis more BBs are added in the median region of the cell than in other regions (antero-posterior gradient of proliferation), and more BBs are added to the ventral rows #n-1, #2 than to the dorsal row #7 (circumferential gradient of BBs proliferation, Kaczanowski 1978). This difference between ventral and dorsal rows in number of BBs was maintained after extensive additional proliferation of BBs within cortical rows, induced by the roscovitine treatment. This additional newly synthesized medial part of cell cortex was added to the forming proter prior to the appearance of the fission zone.

Uncoupling of nuclear divisions and cytokinesis in *Tetrahymena* was induced also by colchicine (Jaeckel-Williams 1978) and was observed in the β-tubulin mutant of *T. thermophila* but the medial positioning of the fission zone was not affected in this mutant (Smith *et al.* 2004). The cells of *cdaK1* thermosensitive mutant also showed an arrest of macronuclear division at the restrictive temperature and when the cells were treated with inhibitor of serine/threonine kinase (6-dimethylaminopurine) at permissive temperature, but after arrest of macronuclear division, the fission zone was shifted anterior. This phenotype was associated with some impairment of component B of epiplasm (Krzywicka *et al.* 1999), what was not observed in this study.

Thus effects of roscovitine on uncoupling of cell division increase of cell size, position and timing of cytokinesis were not a phenocopy of known *Tetrahymena* mutants and were not induced as yet by other treatments.

Putative mechanisms of the posterior shift of the fission zone after roscovitine treatment

Formation of the fission zone in *Tetrahymena* is executed by the introduction of small gaps in the ciliary rows by crosscutting of LMs by the enzyme katanin around the cells equator (Sharma *et al.* 2007). The local activation of the katanin in *Tetrahymena* that is required for the fission zone formation depends upon polyglycylation of β-tubulin in LM's and other posttranslational modifications of microtubules (Fourest-Lieuvin *et al.* 2006, Sharma *et al.* 2007). These data and our data taken together suggest that in the presence of roscovitine newly synthesized medial segments of LMs were not sufficiently modified to be a substrate for katanin action. As a result the fission zone was shifted posterior.

Table 4. The effects of roscovitine on the cell cycle related processes of *T. thermophila*.

Time of cell cycle	Increased
Entry into divisinal morphogenesis	Delayed, at least for 3 h
Stomatogenesis:	
stages I–V	Unaffected
stage VI	Abnormal pattern of oral memmbranells of OA2, number of cells with these abnormality increased with time of treatment
Positioning of the fission line and fission zone	Across of the OA2 or posterior to the OA2
Fission furrow – cytokinesis	Across of OA2 or posterior to OA2, very delayed
Couplets of BBs and ARF	Present, but ARF are often incomplete and abnormaly positioned
Size of dividers	Bigger than untreated cells, proter longer than opisthe
BBs proliferation	Additional proliferation of BBs in ciliary rows during roscovitine induced, cell division delay
Localization of new CVPs in dividing cells	Anterior to the fission zone (as in untreated cells) and/or posterior to the fission zone. One or two sets of new CVPs
Division of macronucleus	Delayed or arrested. If macronucleus did not divide it was localised to proter
Division of micronucleus	Slightly delayed

Effects of roscovitine on the long distance positional information

During normal morphogenesis the new CVPs appear anterior to the fission zone, i.e. in the posterior region of the proter, at the sites determined by their circumferential distance from ciliary row #1 (Nanney 1966, Frankel 2008). This "long distance positional information" was affected by the roscovitine treatment. It is likely that the sites of the new CVPs were displaced due to medial growth of cell cortex in presence of roscovitine, and finally they might belong to the forming opisthe during delayed cell division.

Roscovitine affects the late stages of assembly of oral membranelles and induces asynchrony of BBs involvements in: BBs proliferation along LMs, the OA2 stomatogenesis and in BBs differentiation during fission line formation

The roscovitine affected the late stages of OA2 stomatogenesis inducing aberrant assembly of adoral membranelles. Similar abnormalities in the membranellar pattern in *Tetrahymena* were observed after inhibition of Hsp proteins and impairement of some interaction of the Hsp and tetrins was suggested (Williams and Honts 1987, Honts and Williams 1990, Frankel and Nelsen 2001, Frankel *et al.* 2001, Takeda *et al.* 2001).

Zhang *et al.* (2002) found that all BBs in *Tetrahymena* are associated with the homologue of cyclin-dependent Cdk1 kinase. It is relevant for this discussion that from five antibodies directed against different epitopes of beta-tubulin only one antibody (Tu-06) marked selectively peribasal region of all BBs in ciliary rows, but not in the oral apparatus (Libusova *et al.* 2005). In this study we found that homolog of the Cdc14 phosphatase, another protein implicated in cell cycle regulation and cytoskeleton stability (Cho *et al.* 2005, Ah-Wong and Judelson 2011) is constantly associated with all BBs. Our data on the cdc14 protein, the data of Zang (2002) and Libusova (2005) indicate that some cell cycle regulating proteins and beta-tubulin variants are sequestered by BBs in *Tetrahymena* and it may shed a light in a future on the role of BBs in coordination of cortical morphognesis and other cell cycle pathways.

All these data indicate that during cell cycle of *T. thermophila* the normal morphology of the daughter cells depends on the proper division of micro- and macronucleus and on temporal control of BBs proliferation within the longitudinal (LMs) rows, during OA2 stomatogenesis and during selection of BBs involved in differentiation of apical BBs (couplets) and cell division. The roscovitine induced asynchrony of these processes brings about the array of diverse morphologies of postdivider cells.

Acknowledgements. We thank Dr Malgorzata Kloc for critical reading of the manuscript, Dr Katarzyna Jagusztyn-Krynicka for allowing us to share laboratory rooms, Mrs Marzena Dabrowska for excellent laboratory help, technical and administrative assistance, Dr Elzbieta Wyroba for the usage of Electron Microscopy Facilities of Nencki Institute Poland, Dr Jacek Gaertig for *Tetrahymena thermophila* strain, and Dr Jeff Salibury and Dr Joseph Frankel, and Dr N.E. Williams for the antibodies. We are also thankful for inspiring comments of our reviewers. This study was supported by the grant from the Ministry of Sciences and Higher Education NN 303 091 134 to Dr. J. Dobrzańska-Kaczanowska.

REFERENCES

Ah-Wong A. M. V., Judelson H. S. (2011) New role for Cdc14 phosphatase: Localization to basal bodies in the oomycete *Phytophthora* and its evolutionary coinheritance with eukaryotic flagella. *Plos One* **6**: e16725

Allen R. D. (1967) Fine structures, reconstruction and possible functions of components of the cortex of Tetrahymena pyriformis. *J. Protozool.* **14**: 553–572

Bakowska J., Nelsen E. M., Frankel J. (1982) Development of the ciliary pattern of the oral apparatus of *Tetrahymena thermophila*. *J. Protozool.* **29**: 366–382

Baluska F., Menzel D., Barlow P. W. (2006) Cytokinesis in plant and animal cells: endosomes "shut the door". *Dev. Biol.* **294**: 1–10

Bembenek J., Yu H. (2001) Regulation of the anaphase-promoting complex by the human dual-specificity phosphatase h Cdc14a. *J. Biol. Chem.* **276**: 48237–48242

Bembenek J. N., White J. G., Zheng Y. (2010) A role for separase in the regulation of RAB-11-positive vesicles at the cleavage furrow and midbody. *Curr. Biol.* **20**: 259–264

Brown J. M., Marsala C., Kosoy R., Gaertig J. (1999) Kinesin II is preferentially targeted to assembling cilia and is required for ciliogenesis and normal cytokinesis in *Tetrahymena*. *Mol. Biol. Cell* **10**: 3081–3096

Cho H. P, Liu Y., Gomez M., Dunlap J., Tyers M., Wang Y. (2005) The dual-specificity phosphatase CDC14B bundles and stabilizes microtubules. *Mol. Biol.* **25**: 4541–4551

Cole E., Sugai T. (2012) Developmental progression of *Tetrahymena* through the cell cycle and conjugation. In: *Tetrahymena thermophila*, (Ed. K. Collins). Elsevier AP, 184–237

D'Angiolella V., Mari C., Nocera D., Rametti L., Grieco D. (2003) The spindle checkpoint requires cyclin-dependent kinase activity. *Genes&Devel* **17**: 2520–2525

Diogon M., Henou C., Ravet V., Bouchard P., Vigues B. (2001) Evidence for regional differences in the dynamics of centrin cytoskeletal structures in the polymorphic hymenostome ciliate *Tetrahymena paravorax*. *Eur. J. Protistol.* **37**: 223–231

Eisen J. A., Coyne R. S., Wu M., Wu D., Thiagarajan M., Wortman J. R., Badger J. H., Ren Q., Amadeo P., Jones K. M., Tallon L. J., Delcher *et al.* (2006) Macronuclear genome sequence of the ciliate *Tetrahymena thermophila*, a model eukaryote. *PloS Biol.* **4**: 1620–1642

Fourest-Lieuvin A., Peris L., Gache V., Garcia-Saez I., Juillan-Binard C., Lantez V., Job D. (2006) Microtubule regulation in mitosis: Tubulin phosphorylation by the cyclin-dependent kinase Cdk1. *Mol. Biol. Cell* **17:** 1041–1050

Frankel J., Jenkins L. M., DeBault L. E. (1976) Causal relations among cell cycle processes in *Tetrahymena pyriformis*. An analysis employing temperature-sensitive mutants. *J. Cell Biol.* **71:** 242–260

Frankel J., Nelsen E. M., Martel E. (1981) Development of the ciliature of *Tetrahymena thermophila* II. Spatial subdivision prior to cytokinesis. *Dev. Biol.* **88:** 39–54

Frankel J. (2000) Cell biology of *Tetrahymena*. *Methods Cell Biol.* **62:** 27–125

Frankel J., Nelsen E. M. (2001) The effects of supraoptimal temperatures on population growth and cortical patterning in *Tetrahymena pyriformis* and *Tetrahymena thermophila*: a comparison. *Eukaryot. Microbiol.* **48:** 135–146

Frankel J., Williams N. E., Nelsen E. M., Keeling P. J. (2001) An evaluation of Hsp90 as a mediator of cortical patterning in *Tetrahymena*. *J. Eukaryot. Microbiol.* **48:** 147–160

Frankel J. (2008) What do genic mutations tell us about the structural patterning of a complex single-celled organism? *Eukaryotic. Cell* **7:** 1617–1639

Gonda K., Katoh M., Hanyu K., Watanabe Y., Numata O. (1999) Ca(2+)/calmodulin and p85 cooperatively regulate an initiation of cytokinesis in *Tetrahymena*. *J. Cell Sci.* **112:** 3619–3626

Gonda K., Numata O. (2002) p85 binds to G-actin in Ca++/CaM-dependent manner, thus regulating the initiation of cytokinesis in *Tetrahymena*. *Biochem. Biophys. Res. Comm.* **292:** 1098–10103

Gotesman M., Hosein R. E., Gavin R. H. (2011) MyTH4 independent of its companion FERM domain affects the organization of an intramacronuclear microtubule array and is involved in elongation of the macronucleus in *Tetrahymena thermophila*. *Cytoskeleton* **68:** 220–236

Gould S. B., Kraft L. G. K., van Dooren G. G., Goodman C. D., Ford K. L., Cassin A. M., Bacic A., McFadden G. I., Waller R. F. (2011) Ciliate pellicular proteome identifies novel protein families with characteristic repeat motifs that are common to Alveolates. *Mol. Biol. Evol.* **28:** 1319–1331

Guerra C., Wada Y., Leick V., Bell A., Satir P. (2003) Cloning, localization and axonemal function of *Tetrahymena* centrin. *Mol. Biol. Cell* **14:** 251–261

Heidemann S. R., Kirschner M. W. (1975) Aster formation in eggs of *Xenopus laevis*. Induction by isolated basal bodies. *J. Cell Biol.* **67:** 105–117

Honts J. E., Williams N. E. (1990). Tetrins: Polypeptides that form bundled filaments in *Tetrahymena*. *J. Cell Sci.* **96:** 293–302

Jerka-Dziadosz M. (1981) Cytoskeleton-related structures *in Tetrahymena thermophila:* microfilaments at the apical and division furrow rings. *J. Cell Sci.* **51:** 241–253

Jerka-Dziadosz M., Jenkins L. M., Nelsen E. M., Williams N. E., Jaeckel-Williams R., Frankel J. (1995) Cellular polarities in Ciliates: Persistence of global polarity on a *disorganized* mutant of *Tetrahymena thermophila* that disrupts cytoskeletal organization. *Dev. Biol.* **169:** 644–661

Kaczanowska J., Buzanska L., Ostrowski M. (1993) Relationship between spatial pattern of basal bodies and membrane skeleton (epiplasm) during cell cycle of *Tetrahymena*: *cdaA1* mutant and membrane skeleton immunostaining. *J. Eukaryotic. Microbiol.* **40:** 747–754

Kaczanowska J., Iftode F., Jeanmaire-Wolf R., Clerot J. C., Kiersnowska M., Adoutte A. (1995) Tensegrity model of pattern formation during cytokinesis of a ciliate *Paramecium*-effects of an inhibitor of phosphorylation. *J. Exp. Zool.* **273:** 494–510

Kaczanowska J., Joachimiak E., Buzanska L., Krawczynska W., Wheatley D. N., Kaczanowski A. (1999) Molecular subdivision of the cortex of dividing *Tetrahymena* is coupled with formation of the fission line. *Dev. Biol.* **212:** 150–164

Kaczanowska J., Joachimiak E., Kiersnowska M., Krzywicka A., Golinska K., Kaczanowski A. (2003) The fenestrin antigen in submembrane skeleton of the ciliate *Tetrahymena thermophila* is proposed a marker of cell polarity during cell division and in oral replacement. *Protist* **154:** 251–264

Kaczanowska J., Kaczanowski S., Kiersnowska M., Fabczak H., Tulodziecka K., Kaczanowski A. (2008) Acquisition of cell polarity during cell cycle and oral replacement in *Tetrahymena*. *Int. J. Dev. Biol.* **52:** 249–258

Kaczanowski A. (1978) Gradients of proliferation of ciliary basal bodies and the determination of the position of the oral primordium in *Tetrahymena*. *J. Exp. Zool.* **204:** 417–430

Kaczanowski A., Kiersnowska M. (2011) Inactivation of a macronuclear intra-S-phase checkpoint in *Tetrahymena thermophila* with caffeine affects the integrity of the micronuclear genome. *Protist* **162:** 616–636

Kaiser B. K., Nachury M. V., Gardner B. E, Jackson P. K. (2004) *Xenopus* cdc14 α/β are localized to the nucleolus and centrosome and are required for embryonic cell division. *BMC Cell Bio* 7

Kamijo K., Ohara N., Abe M., Uchimura T., Hosoya H., Lee J.-S., Miki T. (2006) Dissecting the Rho-mediated signaling in contractile ring formation. *Mol. Biol. Cell* **17:** 143–155

Kiersnowska M., Golinska K. (1996) Pattern of phosphorylated structures in morphostatic ciliate *Tetrahymena thermophila*: MPM2 immunogold labeling. *Acta Protozool.* **35:** 297–308

Kirk K. E., Christ C., McGuire J. M, Paul A. G., Vahedi M., Stuart K. R., Cole E. S. (2008) Abnormal micronuclear telomeres lead to an usual cell cycle checkpoint and defects in *Tetrahymena* oral morphogenesis. *Eukaryot. Cell* **7:** 1712–1723

Kovacs P., Pallinger E. (2003) Effects of indomethacin on the divisional morphogenesis and cytoskeleton-dependent processes of *Tetrahymena*. *Cell Biochem. Funct.* **21:** 169–175

Krzywicka A., Kiersnowska M., Wloga D., Kaczanowska J. (1999) Analysis of the effects of the *cdaK1* mutation of *Tetrahymena thermophila* on the morphogenesis of the fission line. *Eur. J. Protistol.* **35:** 342–352

Kushida Y., Nakano K., Numata O. (2011) Amitosis requires gamma-tubulin-mediated microtubule assembly in *Tetrahymena thermophila*. *Cytoskeleton* **68:** 89–96

Lansing T.J., Frankel J., Jenkins L.M. (1985) Oral structure and oral development of the misaligned undulating membrane mutant of *Tetrahymena thermophila*. *J. Protozool.* **32:** 126–139

Libusova L., Sulimenko T., Sulimenko V., Janisch R., Hozak P., Draber P. (2005) Distinct localization of a beta-tubulin epitope in the *Tetrahymena thermophila* and *Paramecium caudatum* cortex. *Protoplasma* **225:** 157–167

Lynn D. H. (1977) Proportional control of organelle position by a mechanism which simultaneously monitors cell size of *wild type* and *conical* form-mutant *Tetrahymena*. *J. Embryol. Exp. Morph.* **42:** 261–274

McDonald B. (1962) Synthesis of deoxyribonucleic acid by micro- and macronuclei of *Tetrahymena pyriformis*. *J. Cell Biol.* **13:** 193–203

Meijer L., Borgne A., Mulner O., Chong J. P. J., Blow J. J., Inagaki N., Inagaki M., Delcros J. G., Moulinoux J. P. (1997) Biochemical and cellular effects of roscovitine, a potent and selective inhibitor of the cyclin-dependent kinases cdc2, cdk2 and cdk5. *Eur. J. Biochem.* **243:** 527–536

Nanney D. L. (1966) Cortical integration in *Tetrahymena*: an exercise in cytogeometry. *J. Exp. Zool.* **161:** 307–317

Nanney D. L. (1975) Patterns of basal body addition in ciliary rows in *Tetrahymena*. *J. Cell Biol.* **65:** 503–512

Nanney D. L. (1982) Genes and phenes in *Tetrahymena*. *BioSci* **32:** 783–788

Nelsen E. M., Frankel J., Martel E. (1981) Development of the ciliature of *Tetrahymena thermophila* I. Temporal coordination with oral development. *Dev. Biol.* **88:** 27–38

Nelsen E. M., Williams N. E,, Yi H., Knaak J., Frankel J. (1994) "Fenestrin" and conjugation in *Tetrahymena thermophila*. *J. Eukaryot. Microbiol.* **41:** 483–495

Numata O., Suzuki H., Ohna H., Watanabe Y. (1995) The mutant gene product of a *Tetrahymena* cell-division-arrest mutant *cdaA* is localized in the accessory structure of specialized basal body close to the division furrow. *Zool. Sci.* **12:** 133–135

Numata O., Gonda K., Watanabe A., Kurasawa Y. (2000) Cytokinesis in *Tetrahymena*: determination of division plane and organization of contractile ring. *Microsc. Res. Tech.* **49:** 127–135

Numata O., Gonda K. (2001) Determination of division plane and organization of contractile ring in *Tetrahymena*. *Cell Struct. Func.* **26:** 593–601

Pearson C. G., Winey M. (2009) Basal body assembly in ciliates: the power of numbers. *Traffic* **10:** 461–471

Queralt E., Uhlmann F. (2008) Cdk-counteracting phosphatases unlock mitotic exit. *Curr. Opin. Cell Biol.* **20:** 661–668

Shang Y., Li B., Gorovsky M. A. (2002) *Tetrahymena thermophila* contains a conventional gamma-tubulin that is differentially required for the maintenance of different microtubule organizing centers. *J. Cell Biol.* **158:** 1195–1206

Shang Y., Tsao C. C., Gorovsky M. A. (2005) Mutational analysis reveal a novel function of the nucleotide-binding domain of γ tubulin in the regulation of basal body biogenesis. *J. Cell Biol.* **171:** 1035–1044

Sharma N., Bryant J., Wloga D., Donaldson R., Davis R. C., Jerka-Dziadosz M., Gaertig J. (2007) Katanin regulates dynamics of microtubules and biogenesis of motile cilia. *J. Cell Biol.* **178:** 1065–1079

Schliva M., Van Blerkom J. (1981) Structural interaction of cytological components. *J. Cell Biol.* **90:** 222–235

Shirayama S., Numata O. (2003) *Tetrahymena* fimbrin localized in the division furrow bundles actin filaments in a calcium-independent manner. *J. Biochem.* **134:** 591–598

Smith J. J., Yakisich J. S., Kapler G. M., Cole E. S., Romero D. P. (2004) A beta-tubulin mutation selectively uncouples nuclear division and cytokinesis in *Tetrahymena thermophila*. *Eukaryot. Cell* **3:** 1217–1226

Steere N., Wagner M., Beishir S., Smith E., Breslin L., Morrison C. G., Hochegger H., Kuriyama R. (2011) Centrosome amplification in CHO and DT40 cells by inactivation of cyclin-dependent kinases. *Cytoskeleton* **68:** 446–458

Stemm-Wolf A. J., Morgan G., Giddings T. H., White E. A., Marchione R., McDonald H. B., Winey M. (2005) Basal body duplication and maintenance require one member of the *Tetrahymena thermophila* centrin gene family. *Mol. Biol. Cell* **16:** 3606–3619

Sugita M., Iwataki Y., Nakano K., Numata O. (2011) Unique sequences and predicted functions of myosins in *Tetrahymena thermophila*. *Gene* **480:** 10–20

Sullivan M., Uhlman F. (2003) A non-proteolytic function of separase links the onset of anaphase to mitotic exit. *Nat. Cell Biol.* **5:** 249–251

Takeda T., Yoshihama I., Numata O. (2001) Identification of *Tetrahymena* hsp60 as a 14-nm filament protein/citrate synthase-binding protein and its possible involvement in the oral apparatus formation. *Genes to Cell* **6:** 139–149

Tavares A., Gonçalves J., Florindo C., Tavares A. A., Soares H. (2012) Mob1: defining cell polarity for proper cell division. *J. Cell Sci.* **125:** 516–527

Thazhath R., Liu C., Gaertig J. (2002) Polyglycylation domain of β-tubulin maintains axonemal architecture and affects cytokinesis in *Tetrahymena*. *Nature Cell Biol.* **4:** 256–259

Thazhath R., Jerka-Dziadosz M., Duan J., Wloga D., Gorovsky M. A., Frankel J., Gaertig J. (2004) Cell context-specific domain on assembly and size of microtubular organelles. *Mol. Biol. Cell* **15:** 4136–4147

TGD (2010) Bradley University LL61625(309):676-7611

Tsou M. F., Wang W. J., Goerge K. A., Uryu K., Stearns T., Jallepalli P. V. (2009) Polo kinase and separase regulate the mitotic lincensing of centriole duplication in human cells. *Dev. Cell* **17:** 344–354

van Leuken R., Clijsters L., van Zon W., Lim D., Yao X., Wolthuis R. M. F., Yaffe M. B., Medema R. H., van Vugt M. A. T. M. (2009) Polo-like kinase1 controls auroraA destruction by activating APC/C-Cdh1. *Plos One* **4:** e 5282

Whittaker S. R., Poele R. H., Chan F., Linardopoulos, Walton M. I., Garrett M. D., Workman P. (2007) The cyclin-dependent kinase inhibitor Seliciclib (R-roscovitine; CYC202) decreases the expression of mitotic control genes and prevents entry into mitosis, *Cell Cycle* **6:** 3114–3131

Wilkes D. E., Otto J. J. (2003) Profilin functions in cytokinesis, nuclear positioning and in stomatogenesis in *Tetrahymena thermophila*. *J. Eukaryot. Microbiol.* **50:** 252–262

Williams N. E., Honts J. E, Graeff R. W. (1986) Oral filaments proteins and their regulation in *Tetrahymena pyriformis*. *Exp. Cell Res.* **164:** 295–310

Williams N. E. (1986) The nature and organization of filaments in the oral apparatus of *Tetrahymena*. *J. Protozool.* **33:** 352–358

Williams N. E., Honts J. E. Jaeckel-Williams R. F. (1987) Regional differentiation of the membrane skeleton in *Tetrahymena*. *J. Cell Sci.* **187:** 457–463

Williams N. E., Honts J. E. (1987) The assembly and positioning of cytoskeletal elements in *Tetrahymena*. *Development* **100:** 23–30

Williams N. E., Honts J. E., Kaczanowska J. (1990) The formation of basal body domains in the membrane skeleton. *Development* **109:** 935–942

Williams N. E., Honts J. E., Dress V. M., Nelsen E. M., Frankel J. (1995) Monoclonal antibodies reveal complex structure in the membrane skeleton of *Tetrahymena*. *J. Euk. Microbiol.* **42:** 422–427

Williams N. E., Tsao C. C., Bowen J., Hehman G. L., Williams R. J., Frankel J. (2006) The actin gene ACT1 is required for phagocytosis, motility and cell separation of *Tetrahymena thermophila*. *Eukaryot. Cell* **5:** 555–56728

Wu J., Cho H. P., Rhee D. B., Johnson D. K., Dunlap J., Lio Y., Wang Y. (2008) Cdc14B depletion leads to centriole amplifi-

cation, and its overexpression prevents unscheduled centriole duplication. *J. Cell. Biol.* **181:** 475–483

Wu M., Allis D., Gorovsky M. A. (1988) Cell-cycle regulation as a mechanism for targeting proteins to specific DNA sequences in *Tetrahymena thermophila*. *Proc. Natl. Acad. Sci. USA* **85:** 2205–2209

Yasuda T., Numata O., Ohnishi K., Watanabe Y. (1980) A contractile ring and cortical changes found in the dividing *Tetrahymena pyriformis*. *Exp. Cell Res.* **128:** 407–417

Zhang H., Huang X., Tang L., Zhang Q. J., Frankel J., Berger J. D. (2002) A cyclin-dependent protein kinase homologue associated with the basal body domains in the ciliate *Tetrahymena thermophila*. *Biochim. Biophys. Acta* **1591:** 119–128

Zineldeen D. H., Shimada M., Niida H., Katsuno Y., Nakanishi M. (2009) Ptpcd-1 is a novel cell cycle related phosphatase that regulates centriole duplication and cytokinesis. *Biochem. Biophys. Res. Com.* **380:** 460–466

Zweifel E., Smith J., Romero D., Giddings T. H., Winey M., Honts J., Dahlseid J., Schneider B., Cole E. S. (2009) Nested genes CDA12 and CDA13 encode proteins associated with membrane trafficking in the ciliate *Tetrahymena thermophila*. *Eukaryotic Cell* **8:** 899–912

Received on 6th March, 2012; Revised on 14th May, 2012; Accepted on 24th May, 2012